Jiniraj et al. 2021. *Int. J. Vehicle Structures & Systems*, 13(1), 97-101
ISSN: 0975-3060 (Print), 0975-3540 (Online)
doi: 10.4273/ijvss.13.1.19

International Journal of Vehicle Structures & Systems
Available online at www.maftree.org/eja

Aerodynamic Investigation of Morphing Wing UAV with Adjustable Slotted Airfoil Configuration

R. Jiniraj[a], R. Venkat Raman[b] and N. Dinesh[c]

Dept. of Aeronautical Engg., Er. Perumal Manimekalai Engg. College, Hosur, Tamil Nadu, India
[a]Corresponding Author, Email: jinirajaero@gmail.com
[b]Email: venkat03raman@gmail.com
[c]Email: dineshmrf10@gmail.com

ABSTRACT:

Aviation has wide aspects to challenge and discover, the ability to land and take off at slow speed, sudden increase in drag for short runway landings. This paper puts forth the solution by the use of adjustable multi slots configuration of an airfoil. In this case, the slots extend from the wing leading edge to trailing edge. This causes change in the chord, thereby changing the camber of unsymmetrical airfoil. An investigation was made to determine and compare the aerodynamic characteristics of multi slotted adjustable airfoil with un-morphed unsymmetrical airfoil at varied speeds and Angle of Attack (AoA). There are three slots distanced equally along the airfoil. The extension of these slots increases the chord length by 10% of total chord. The slotted and un-slotted airfoil profile are then studied using computational fluid dynamics of external flow over a body. The flow simulation is done at 10m/s, 20m/s, 30m/s, 40m/s and 50 m/s flow velocity and at 0, 3, 6, 9 ,12, 15 AoA. The results were obtained for each case and the values for base and slotted model were compared. It was found that lift of slotted model is slightly higher than base model at low flow velocity. It was also seen that the use of slots at high speed causes a large amount of drag. This increased drag factor can be used in UAV's as spoilers during landing or for landing at shorter runways at lower speed, allowing a sudden decrease in aircraft speed and also to glide at a steeper angle over obstruction.

KEYWORDS:

Adjustable multi slots; Unmorphed unsymmetrical airfoil; Flow simulation; Spoilers; Steeper angle

CITATION:

R. Jiniraj, R.V. Raman and N. Dinesh. 2021. Aerodynamic Investigation of Morphing Wing UAV with Adjustable Slotted Airfoil Configuration, *Int. J. Vehicle Structures & Systems*, 13(1), 97-101. doi:10.4273/ijvss.13.1.19.

1. Introduction

Morphing is the altering or changing of the shape in order to alter its performance characteristics. The maximum lift co-efficient was obtained with a highly cambered fixed slotted airfoil but the minimum drag co-efficient of the arrangement was high. This paper presents the aerodynamic investigation of morphing wing UAV with adjustable slotted airfoil. The airfoil can be actively morphed by extending and closing the slots [1]. Base model used for the study and morphing is NACA 4412, an unsymmetrical airfoil, which allows the change of camber by altering the total chord of airfoil. The slotted airfoil investigated in this paper has four slots distanced equally along the chord. This passive morphing of airfoil is done using telescopic mechanism. It alters the profile of airfoil, there by changing its aerodynamic performance. Base profile and altered profile are then simulated in ANSYS FLUENT. Fred et al [2] tested different combination of slots to determine the change in aerodynamic characteristics of equipping a Clark Y airfoil with four fixed slots and a trailing edge flap. Different slots combination has been analysed for maximum lift co-efficient to obtain the optimum combination. The same combinations have also been analysed for rear flap tilted down by 45°. Lift and drag test were made on Clark Y wing in 5-foot vertical wind tunnel of the NACA. Improvement of the aerodynamic performance of NACA 4412 using adjustable airfoil profile during the flight was examined by Ibrahim et al [3]. The highlights of this paper were the investigation of stall parameter, performance of the drag and lift force analysis and the design of adjustable airfoil profile. Maki et al [4] performed an experimental study on morphing wing configuration with multi-slotted variable camber mechanism. A designated segment of the base wing is divided into overlapped five-elemental wings with a shorter chord length 1. The slots can be spread or closed to adjust the camber of overall wing. The mechanism proposed has a single motor and a linkage system.

Beguin et al [5] assessed the aerodynamic optimization of a morphing membrane wing where the passive deformation of the membrane is controlled by varying its pre-tension. This method effectively allows to adjust the camber of the wing within certain range at a given flow condition. Aircraft flight performance can be increased by optimizing the wing design. However, fixed wing design has disadvantages since the aircraft's wing unable to achieve maximum flight performance in all flight condition. Thus, the wing shape demanded to evolve or change with view to adapt with different flight condition by Zaini et al [6]. Different airfoil shape

change improves the aerodynamics of the wing. Slotted airfoil shape also increases the camber of airfoil. Kondapalli et al [7] investigated on the characteristics of airfoil during shape optimization. Juan et al [8] investigated on slotted wing by implementing fixed slots along the span of the wing and found increase in aerodynamic performance.

Wenzinger et al [9] calculated the aerodynamic characteristics of the wing depending on airfoil slot position and found that it will generate the greatest increase in maximum lift co-efficient. Shortal et al [10] found slots show great influence on the lateral stability and can be controled by maintaining the wing controls during flight at high AoA. Weick et al [11] stated that fixed rectangular slotted wings behaviour at high AoA, by slots the chord is changed in airfoil. Chord morphing reduces the drag generated on wing [12]. By chord morphing aerodynamics performances like lift coefficient and lift to drag ratio is increased [13]. Chord morphing on wing replaces conventional ailerons usage [14]. Sun et al [20] investigated on the boundary layer effect of multiple slotted airfoils and show how to control boundary layer separation. Whitman et al [21] offered a detailed design geometry of the slot. The aerodynamic analysis of NACA 4412 airfoil is done by Kevadiya et al [27]. This paper presents the aerodynamic analysis and performance of NACA 4412 airfoil with slots and without slots.

2. Slotted airfoil design and meshing

The airfoil model considered for investigation is a two-dimensional (2D) NACA 4412 airfoil. The aerodynamic characteristics of NACA 4-series airfoil at different Reynolds's number were taken from the standard data. Another geometry considered for investigation is a morphed model of NACA 4412. The morphed model has three adjustable slots dividing the airfoil in four equal sections. This alters the chord length depending on the operation. The distance of each slots were referred from Weick et al [3] report of multi-slotted Clark Y airfoil. Fig. 1(a) represents the NACA 4412 airfoil of 1m chord length. Fig. 1(b) represents the slotted NACA 4412 airfoil [26] and it has 3 slots of equal distance of 0.1m. Hence, the chord of slotted airfoil is increased to 1.3m considering the gap between each slot as 0.1m.

Fig. 1(a): NACA 4412 airfoil

Fig. 1(b): Slotted NACA 4412 airfoil

Meshing of the slotted and the base model is done by means of ANSYS meshing software tool. Curvilinear grid is chosen for meshing the airfoil section. Hybrid mesh is created with fine mesh near the airfoil in order of 0.01 to get accurate and precise flow values. Hybrid mesh has both structured mesh and unstructured mesh. Structured mesh is done around the airfoil to get precise values and unstructured mesh [22] is done apart from the airfoil. The meshing has total 210055 nodes and 208794 elements. Body of influence is done at different condition they are 0.01, 0.0075 and 0.005 to get the efficient flow analysis and accurate flow values. Inflation is also carried out with this of 15 layers and constant growth rate of 1.2 were used for inflation option as shown in Fig. 2(a). Edge sizing is also done and the airfoil was divided into 1000 segments. Grid independence study [16] results are given in Table 1.

Table 1: Grid independence study results for NACA 4412 airfoil

Elm. length, m	Elements	Nodes	ΔC_l	ΔC_d
0.01	208794	210055	0.42616	0.011132
0.0075	355489	356775	0.41643	0.011658
0.005	771192	772482	0.39733	0.01284

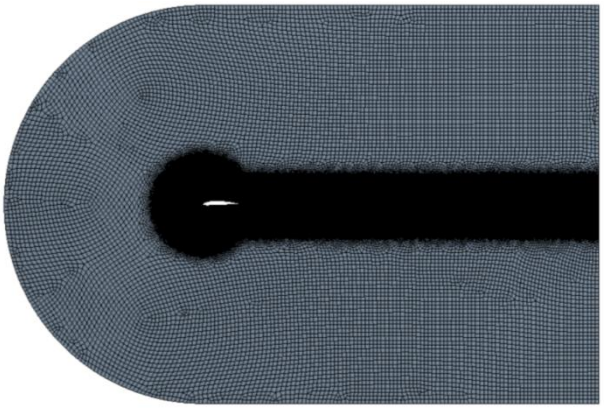

Fig. 2(a): Meshed airfoil (NACA 4412) and CFD domain

Fig. 2(b) represents NACA 4412 meshed airfoil with different boundary condition, body sizing, edge sizing and inflation to get the precise values and accurate results. Maximum face sizing is 0.1m and the same is given for the maximum face thickness. In the body sizing, the element sizes considered are 0.01, 0.0075 and 0.005. The airfoil is divided into 1000 equal parts in edge sizing. Finally, inflation for the airfoil is investigated with 15 layers. Fig. 2(c) represents slotted NACA 4412 meshed airfoil. Primarily it is divided into 4 parts comprising of 3 slots. The slots separated by an equidistance of 0.1m, are also meshed under body sizing, edge sizing, and inflation. In body sizing maximum face sizing and thickness as 0.01m. In edge sizing, the airfoil is divided into 1000 equal parts comprising 200, 300, 300 and 150 segments respectively for the 1st, 2nd, 3rd and 4th part of the slotted airfoil. Finally, inflation for the airfoil is investigated with 15 layers

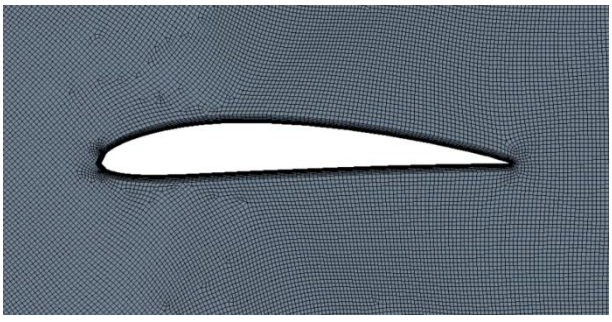

Fig. 2(b): NACA 4412 meshed airfoil

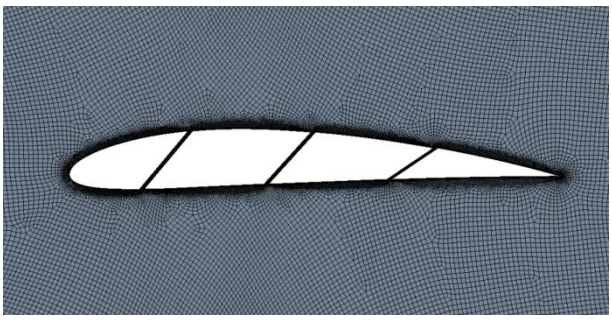

Fig. 2(c): Slotted NACA 4412 meshed airfoil

3. CFD simulations

Ansys Fluent [15, 24] is used to study the effect of slots in the airfoil. The solver settings are 2D external flow, double precision and Spalart-Almaras turbulence model [23, 25]. The simulations of un-slotted and slotted NACA 4412 airfoil are carried out for pressure based steady state condition [28-30]. The results are observed for 10m/s, 20m/s, 30m/s, 40m/s and 50m/s flow velocity at 0°, 3°, 6°, 9°, and 12° AoA respectively. The applied boundary conditions are velocity inlet, pressure outlet and boundary wall for the far field and airfoil domains. Fig. 3(a) and 3(b) show the static pressure contours for the un-slotted airfoil simulations at 10m/s and 50 m/s velocities. The static pressure varies from 42.9Pa to 57.9Pa and -1170Pa to 1460Pa respectively at 10m/s and 50 m/s. The difference in pressure at the upper surface is around 1.41% and 1.247% respectively at 10m/s and 50 m/s. When the altitude increases, the pressure decreases gradually. The static pressure is concentrated at the leading edge of airfoil compared to the top surface of the un-slotted NACA 4412 airfoil.

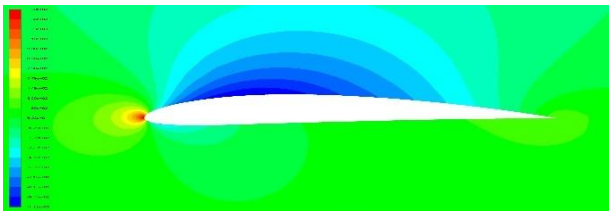

Fig. 3(a): Static pressure contour at 10 m/s – Un-slotted airfoil

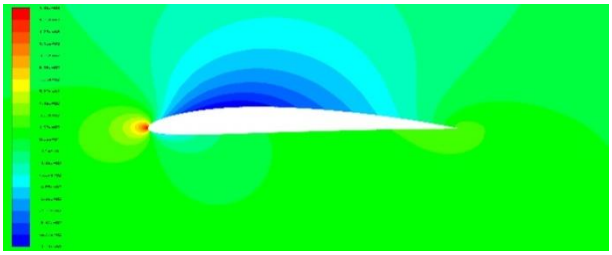

Fig. 3(b): Static pressure at 50 m/s – Un-slotted airfoil

Fig. 4(a) and 4(b) show the velocity contour of the base model for the simulations at 10m/s and 50 m/s velocities. At 10 m/s, the velocity varies from -0.0204m/s to 13m/s. The velocity is uniformly distributed at the leading and trailing edges of the airfoil. At 50 m/s, the velocity varies from 0m/s to 66.4m/s. The velocity is concentrated at the top surface of airfoil due to low pressure. When the pressure decreases, the velocity will increase automatically since the velocity is inversely proportional to the pressure.

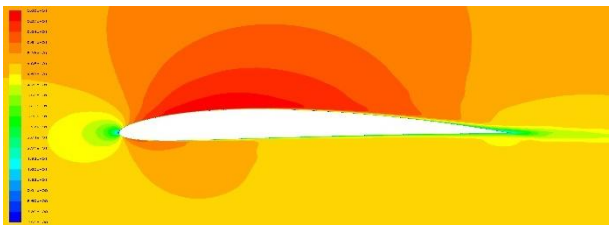

Fig. 4(a): Velocity contour of the base model at 10 m/s

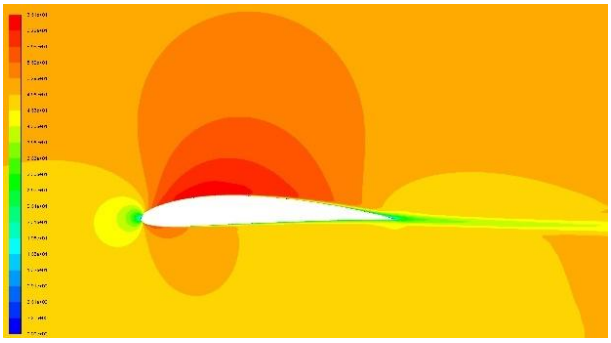

Fig. 4(b): Velocity contour of the base model at 50 m/s

Fig. 5(a) depicts that the static pressure is varying from -1760Pa to 1500Pa for the slotted airfoil at 10m/s. The difference in pressure is around 1.173%. The static pressure is concentrated at the leading edge of airfoil when compared to the top surface of the slotted airfoil. Fig. 5(b) depicts that the velocity is varying from -15.8m/s to 63.4 m/s for the slotted airfoil at 10m/s. The velocity is concentrated at the top surface and at the bottom of the leading edge due to high pressure at the leading edge of the slotted airfoil. The difference in velocity will be 4.012% compared with base model velocity at 10m/s. The velocity is minimum between the slots and top of the trailing edge of the slotted airfoil.

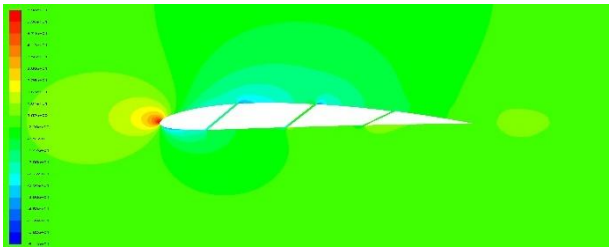

Fig. 5(a): Static pressure contour at 10 m/s – Slotted airfoil

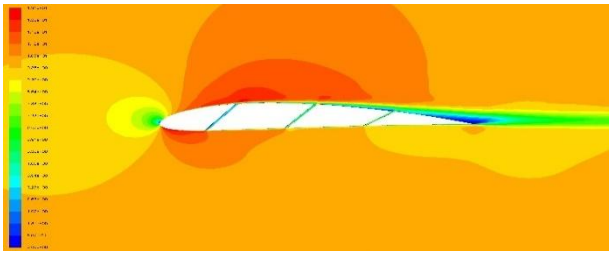

Fig. 5(b): Velocity contour at 10 m/s - Slotted airfoil

4. Results and discussion

Graphic contours and XY plot obtained from different cases of simulation are studied. The flow velocity, static pressure, pressure co-efficient, lift co-efficient and drag co-efficient with respect to AoA were noted for base model and slotted model. The results obtained from computational flow field analysis at different velocities

and different AoA [17-19] are considered for further assessment. Fig. 6 shows the variation of Cl for a range of AoA at 10 m/s. C_l of the slotted airfoil has gradually increased from 0 to 6° AoA after wards it decreases gradually due to stalling angle and slots in the airfoil. C_l for un-slotted NACA 4412 airfoil has progressively increased up to 15° AoA. Slotted airfoil has produced high lift compared with the base model airfoil from 0 to 6° AoA. Therefore, slotted airfoil has optimum lift than the base model airfoil at lower AoA but at higher AoA the base model airfoil dominates the lift performance.

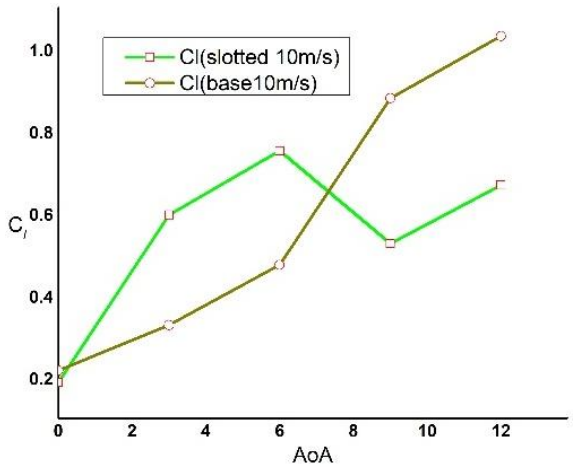

Fig. 6: Coefficient of lift vs. AoA at 10 m/s

Fig. 7 shows that the drag of slotted airfoil has decreased by 0.05% compared with base model at 10 m/s. C_d of slotted airfoil has decreased up to 6° AoA and then increased suddenly up to 9° AoA and thereafter reduced again. This is due to the existence of slots in airfoil and by the formation of vortices in between the slots which tend to push the airfoil backwards. Due to wake formation at 6° AoA, more drag was generated suddenly.

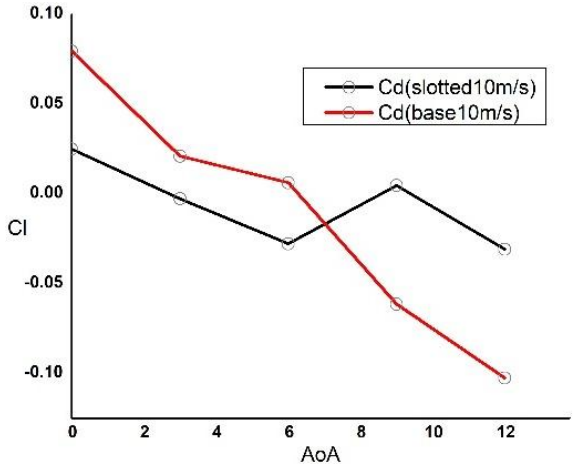

Fig. 7: Coefficient of drag vs. AoA at 10 m/s

C_l and C_d distribution of airfoil is due to pressure difference created around the airfoil. Fig. 8 and 9 show the co-efficient of pressure (Cp) along the chord length for the un-slotted airfoil and slotted airfoil respectively at 50 m/s. For un-slotted airfoil, the C_p peaks at the lower surface of the airfoil and drops at the upper surface of the airfoil. NACA 4412 airfoil lower surface is cusped at trailing edge. This causes the flow to slow down near the cusped region of airfoil lower surface. Velocity is inversely proportional to pressure. Therefore, the co-efficient of pressure is high at the lower surface and low at the upper surface for un-slotted airfoil. Due to the gap between each slot, the flow slows down between the slots and it is increased at airfoil parts as shown in Fig. 9 for the slotted airfoil. The maximum C_p is noticed at Part 1. The C_p of the lower surface at the 1st slot is at 0.05. C_p was constant at second and third slots and C_p is about 0.7 thereafter. C_p peaks heavily to maximum at the lower surface of airfoil and drops at the slots of slotted airfoil. The C_p drops down heavily due to the formation of high pressure associated with the presence of slots between the airfoil surfaces.

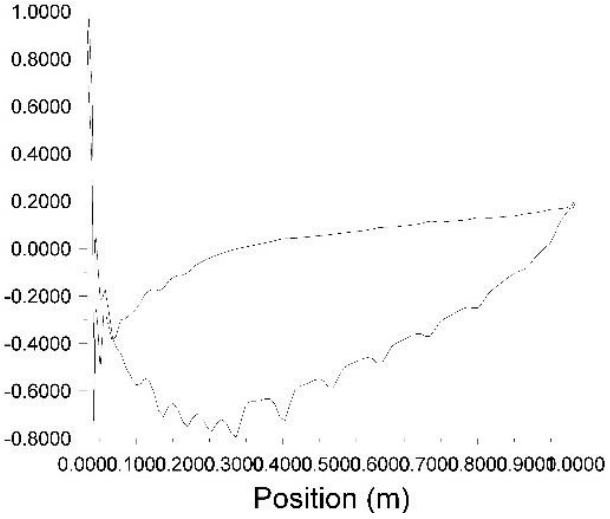

Fig. 8: Cp at 50m/s - Un-slotted airfoil

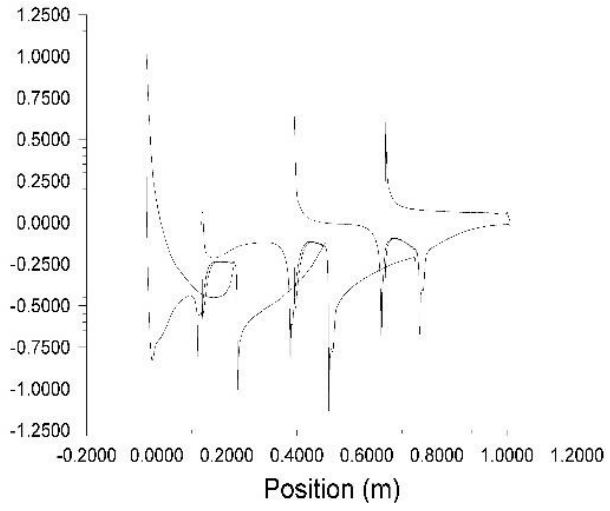

Fig. 9: Cp at 50 m/s – Slotted airfoil

5. Conclusion

The Aerodynamic investigation of two dimensional NACA 4412 airfoil and adjustable slotted airfoil configuration was performed and results were compared. This morphing technique done using adjustable slotted configuration is employed to alter the chord and camber of the airfoil during flight. It was noted that the use of these slots on an aircraft is to land at lower speed at shorter runways. During investigation it was assessed

that the lift increases slightly due to the presence of slots at low speed (10m/s) at low AoA. Hence, slotted airfoils can effectively be used for the wings of the UAVs.

REFERENCES:

[1] G. Lachmann. 1924. *Results of Experiments with Slotted Wings*, TM No. 282, NACA, Washington, DC, US.

[2] F. Weick and J. Wezinger. 1932. *The Effect of Multiple Fixed Slots and a Trailing Edge Flap on The Lift and Drag of a Clark Y Airfoil*, Report No. 427, NACA, Washington, DC, US.

[3] I. Kabin, M.H. Dogru and U. Korkmaz. 2018. Improvement of the aerodynamic performance of NACA 4412 using the adjustable airfoil profile during the flight, *J. Faculty of Engg. and Architecture of Gazi University*, 34(2), 1109-1125. https://doi.or./10.17341/gazimmfd. 460536.

[4] M. Maki and D. Hirabayashi. Experimental study of a morphing wing configuration with multi-slotted variable-camber morphing, *Proc. AIAA Atmospheric Flight Mechanics Conf.*, Washington, D.C. https://doi.org/10.2514/6.2016-3849.

[5] B. Beguin, C. Breitsamter and N. Adams. 2012. Aerodynamic optimization of a morphing membrane wing, *Proc. 28th Int. Congress of the Aerodynamic Sci. 2012*, 1168-1178, Brisbane, Australia.

[6] H. Zaini and N.I. Ismail. 2016. A review of morphing wing, *Mech. Engg. Colloquium*, 1-6.

[7] Kondapalli. 2013. Aerofoil Profile Analysis and Design optimization, *J. Aerospace Engg. and Tech.*, 3(2). https://doi.org/10.37591/.v3i2.656.

[8] J.F. Granizo. 2016. *Effect of Slot Span on Wing Performance*, MS. Aerospace Engg. Thesis, Embry Riddle Aeronautical University, Florida.

[9] C. Wenzinger and J. Shortal. 1931. *The Aerodynamic Characteristics of a Slotted Clark Y Wing as Affected by the Auxiliary Airfoil Position*, TR No. 400, NACA, Washington, DC, US.

[10] F. Weick and J. Shortal. 1932. *The Effect of Multiple Fixed Slots and a Trailing-Edge Flap on the Lift and Drag of a Clark Y Airfoil*, Report No. 427, NACA, Washington, DC, US.

[11] F. Weick and C. Wenzinger. 1932. *Effect of Length of Handley Page Tip Slots on the Lateral-Stability Factor, Damping in Roll*, TN. No. 423, NACA, Washington, DC, US.

[12] C. Thill, J.A. Etches, I.P. Bond, K.D. Potter and P.M. Weaver. 2010. Composite corrugated structures for morphing wing skin applications, *Smart Mater. Struct.*, 19(12), 124009. https://doi.org/10.1088/0964-1726/19/ 12/124009

[13] O. Bilgen and M.I. Friswell. 2014. Piezoceramic composite actuators for a solid-state variable-camber wing, *J. Intell. Mater. Syst. Struct.*, 25(7), 806-817. https://doi.org/10.1177/1045389X13500575.

[14] F. Previtali, G. Molinari, A.F. Arrieta, M. Guillaume and P. Ermanni. 2015. Design and experimental characterisation of a morphing wing with enhanced corrugated skin, *J. Intell. Mater. Syst. Struct.*, 27(2), 278-292. https://doi.org/10.1177/1045389X15595296.

[15] *FLUENT - User Guide*. 2006. Spalart-Allmaras Model Theory, Fluent Inc.

[16] LEAP CFD Team. 2015. *Convergence and Mesh Independence Study*. URL:http://www.computational fluiddynamics.com.au/convergence-and-meshindependent-study/

[17] L.J. Clancy. 1980. *Aerodynamics*, Arnold-Heinemann Pub., Great Britain.

[18] E.L. Houghton and P.W. Carpenter. 2003. *Aerodynamics for Engg. Students*, 5th Ed., Butterworth Heinmann, UK.

[19] J.D. Anderson Jr. 2001. *Fundamentals of Aerodynamics*, 3rd Ed., McGraw Hill, UK.

[20] M. Sun and H. Hamdani. 2001. Separation control by alternating tangential blowing/suction at multiple slots - Technical Note, *AIAA J.*, 39(4), 735-736. https://doi.org/ 10.2514/2.1369.

[21] N. Withman, R. Sparks, S. Ali and J. Ashworth. 2006. Experimental investigation of slotted airfoil performance with modified slot configurations, *Proc. 24th AIAA Applied Aerodynamics Conf.*, Embry-Riddle Aeronautical University, San Francisco, California. https://doi.org/10.2514/6.2006-3481.

[22] G. Bono and A.M. Awruch. 2007. Numerical study between structured and unstructured meshes for Euler and Navier-Stokes equations, *Argentinian Association of Computational Mechanics*, 26, 3134-146.

[23] Wilcox and David. 1998. *Turbulence Modeling for CFD*, 2nd Ed., Anaheim, California.

[24] G. Batchelor. 1967. *An Introduction to Fluid Dynamics*, Cambridge University Press, UK.

[25] P.R. Spalart and S.R. Allmaras. 1994. A one-equation turbulence model for aerodynamic flows, *Aerospace Research*, 1, 5-21.

[26] http://airfoiltools.com/polar/details?polar=xf-naca4412-il-50000-n5, 2018.

[27] M. Kevadiya and H.A. Vaidya. 2013. 2D analysis of NACA 4412 airfoil, *Int. J. Innovative Research in Sci., Engg. and Tech.*, 2(5), 1686-1691.

[28] T.L. Holst. 1994. *Computational Fluid Dynamics Uses in Fluid Dynamics/Aerodynamics Education*, NASA Tech. Memorandum, 108834.

[29] S. Hossain, M.F. Raiyan, M.N.U. Akanda and N.H. Jony. 2014. A comparative flow analysis of NACA 6409 and NACA 4412 aerofoil, *Int. J. Research in Engg. and Tech.*, 3(10), 1-9. https://doi.org/10.15623/ijret.2014. 0310055.

[30] K.S. Patel, SB. Patel, U.B. Patel and A.P. Ahuja. 2014. CFD analysis of an aerofoil, *Int. J. Engg. Research*, 3(3), 154-158. https://doi.org/10.17950/ijer/v3s3/305.